

Old Dominion University ODU Digital Commons

CCPO Publications

Center for Coastal Physical Oceanography

11-2000

Inference of Tidal Elevation in Shallow Water Using a Vessel-Towed Acoustic Doppler Current Profiler

Chunyan Li

Arnoldo Valle-Levinson
Old Dominion University

Larry P. Atkinson
Old Dominion University, latkinso@odu.edu

Tom C. Royer
Old Dominion University

Follow this and additional works at: https://digitalcommons.odu.edu/ccpo_pubs

 Part of the [Oceanography Commons](#)

Repository Citation

Li, Chunyan; Valle-Levinson, Arnoldo; Atkinson, Larry P.; and Royer, Tom C., "Inference of Tidal Elevation in Shallow Water Using a Vessel-Towed Acoustic Doppler Current Profiler" (2000). *CCPO Publications*. 100.
https://digitalcommons.odu.edu/ccpo_pubs/100

Original Publication Citation

Li, C.Y., Valle-Levinson, A., Atkinson, L.P., & Royer, T.C. (2000). Inference of tidal elevation in shallow water using a vessel-towed acoustic Doppler current profiler. *Journal of Geophysical Research-Oceans*, 105(C11), 26,225-26,236. doi: 10.1029/1999jc000191

This Article is brought to you for free and open access by the Center for Coastal Physical Oceanography at ODU Digital Commons. It has been accepted for inclusion in CCPO Publications by an authorized administrator of ODU Digital Commons. For more information, please contact digitalcommons@odu.edu.

Inference of tidal elevation in shallow water using a vessel-towed acoustic Doppler current profiler

Chunyan Li

Skidaway Institute of Oceanography, Savannah, Georgia

Arnoldo Valle-Levinson, Larry P. Atkinson, and Tom C. Royer

Center for Coastal Physical Oceanography, Department of Ocean, Earth, and Atmospheric Sciences, Old Dominion University, Norfolk, Virginia

Abstract. Vessel-towed acoustic Doppler current profilers (ADCPs) have been widely used to measure velocity profiles. Since the instrument is usually mounted on a catamaran floating on the surface, previous studies have used the water surface as the reference level from which the vertical coordinate for the velocity profile is defined. However, because of the tidal oscillation, the vertical coordinate thus defined is time-dependent in an Earth-coordinate system, which introduces an error to the estimated harmonic constants for the velocity. As a result, the total transport will also be in error. This is particularly a problem in shallow waters where the tidal elevation is relatively large. Therefore tidal elevation needs to be resolved to make a correct harmonic analysis for the velocity. The present study is aimed at resolving the tidal elevation change in shallow water using a vessel-towed ADCP. Semidiurnal and diurnal tidal elevations across the lower Chesapeake Bay have been determined using a vessel-towed ADCP. Data from four cruises ranging from 25 to 92 hours in 1996 and 1997 are used. Water depth averaged every 30 s by the ADCP is studied by harmonic and statistical analysis. By selecting only the data within a narrow band (~ 320 m) over the planned transect, we are able to improve the reliability of the data. We then grid the depth data along the 16 km transect into 200 equal segments and use harmonic analysis to resolve the semidiurnal and diurnal tidal variations within each segment. We find that (1) the depth data from the ADCP contain both semidiurnal and diurnal signals that can be resolved, from which the surface elevation can be inferred, (2) the major error appears to come from spatial variation of the depth, (3) the semidiurnal and diurnal tidal variations of elevation inferred over flat bottom topography account for almost 100% of the total variability, while those measurements over large bottom slopes account for a much lower percentage of the total variability, (4) at least 70% of the variability of depth can be explained by semidiurnal and diurnal tides if the bottom slope is smaller than 0.006, and (5) the spatial variation of both amplitude and phase of the elevation along the transect appears to be small with a slightly lower tidal amplitude at the south of the Chesapeake Bay entrance, consistent with the Coriolis effect. The inferred elevations from the ADCP readings are consistent with sea level measurements at a tide station 10 km inside the estuary.

1. Introduction

Vessel-towed acoustic Doppler current profilers (ADCPs) have been frequently used to measure water velocity in shallow estuaries and coastal waters [e.g., *Lwiza et al.*, 1991; *Valle-Levinson et al.*, 1998; *Brubaker and Simpson*, 1999]. The ADCP is usually mounted on a

catamaran floating on the surface and towed at one side of a vessel [*Valle-Levinson et al.*, 1998]. Tidal velocity harmonics as well as the residual velocity components can be obtained from these measurements. An effective method is to repeatedly sample the velocity profile along a transect over at least one tidal cycle. The harmonic constants can be resolved if multiple measurements (e.g. eight or more) are made during one tidal period. Since the instrument is towed on the surface, these studies have used the water surface as the reference level from which the vertical coordinate for the velocity profile is determined. This is convenient and

Copyright 2000 by the American Geophysical Union.

Paper number 1999JC000191.
0148-0227/00/1999JC000191\$09.00

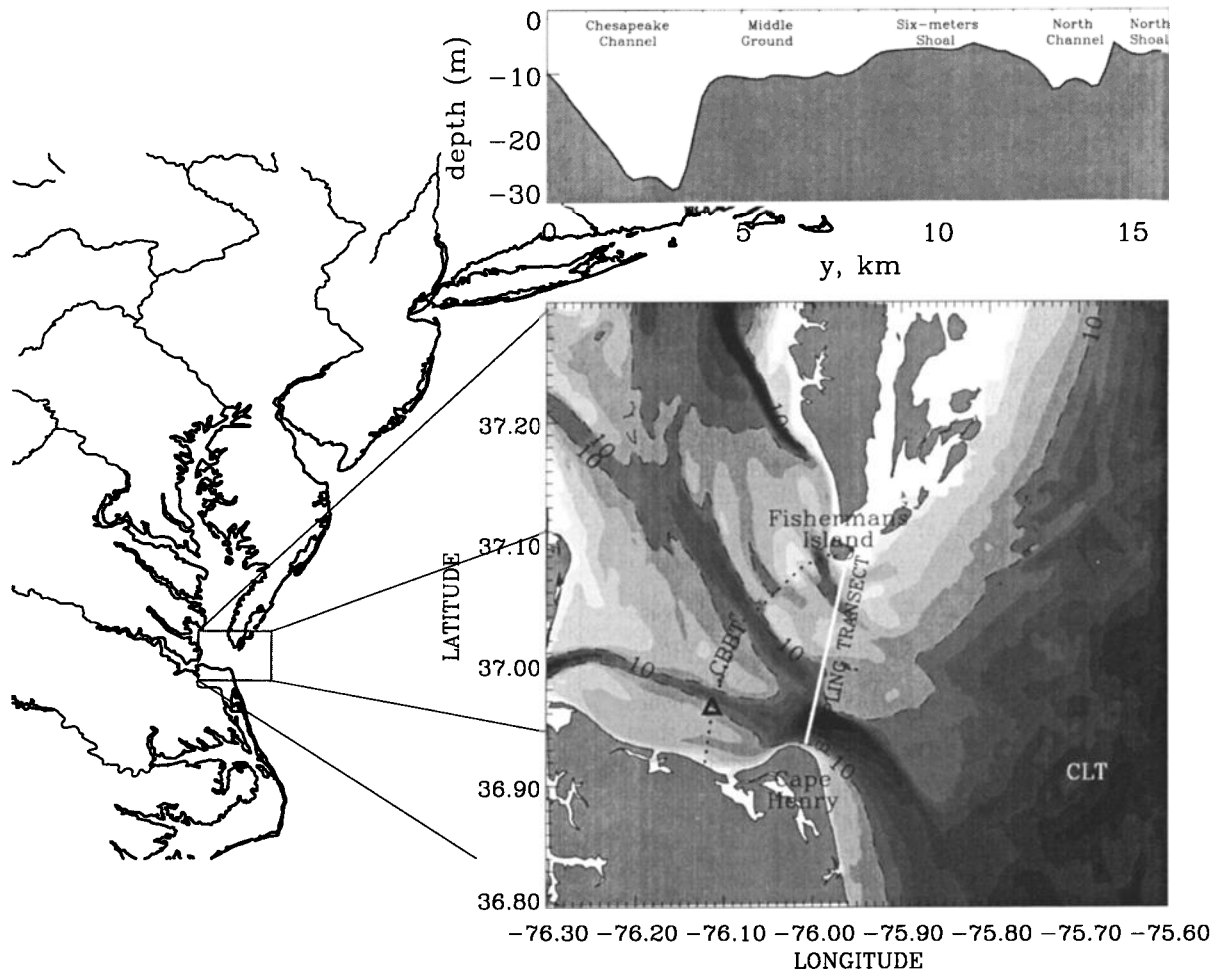


Figure 1. Study area and sampling transect along which the ADCP was towed by NOAA's ship *Ferrel*. The upper right graph shows the mean depth along the transect.

no coordinate transformation in the vertical is needed. However, the water surface is constantly changing, because of the tidal oscillation. The vertical coordinate is then time-dependent relative to a fixed bottom, which will introduce an error to the estimated harmonic constants for the velocity profiles. This is especially true over shallow water such as at the Chesapeake Bay entrance, where the water is mostly shallower than 12 m with a maximum depth of about 30 m (Figure 1) and the tidal range can reach 1.5 m. Therefore tidal elevation needs to be resolved in order to do a vertical coordinate transformation and to make a correct harmonic analysis for the velocity in an Earth-coordinate system. By resolving the tidal elevation, a "fixed" level, such as the mean sea level, can be clearly defined as the reference level. An ideal situation would be (1) the vessel precisely follows the planned transect during each repetition, or (2) the mean water depth is constant. Under one of these conditions, the bottom can be used as a reference level with no difficulty. In reality, the water depth changes in space and the vessel usually traverses slightly different lines during different repetitions and does not arrive exactly at a given position. The depth

variability due to this (often random) position shift can be greater than the range of the tidal elevation in the area, which will prevent inference of the water surface variation from the measured depth. This could be another reason why previous studies have ignored the water surface elevation and have not used a fixed level as the reference for the vertical coordinate.

Tidal elevation information is useful for more than the above discussed vertical coordinate transformation. An example is vertically integrated transport calculations. The vertically integrated transport through a vertical section of unit width during one tidal period is [Phillips, 1977]

$$M = \overline{\int_{-h}^{\zeta} u dz} = \int_{-h}^{-a} \bar{u} dz + \overline{\zeta u|_{z=\zeta}}, \quad (1)$$

in which ζ , a , h , u , and z are the instant surface elevation, amplitude of the tide, mean water depth, horizontal velocity perpendicular to the vertical section, and the vertical coordinate (positive upward with the origin at the mean sea level), respectively. Note that the vertical integration of horizontal velocity in (1) has

been expressed by an integration from the bottom to the trough of the tidal wave ($z = -a$) and an integration from the trough to the surface. Note also that in (1), u is defined to be zero where there are no particles (i.e., above the surface or where $z > \zeta$). Many previous studies [e.g., Ianniello, 1977] used $z = 0$ instead of $z = -a$ for the integration, while in reality there is no water above the surface [Li and Fang, 1999]. The elevation ζ is defined to be zero at the mean sea level ($z = 0$). The overbar denotes a time average. The first term on the right-hand side of (1) is not directly related to the surface elevation. The second term on the right-hand side of (1) is obviously dependent on the surface elevation and is important unless the phase difference between ζ and u is 90° (a standing wave) or the mean water depth h is much larger than the tidal amplitude a . Therefore the information concerning tide is essential in determining the water mass (and other material) transport and the dominant mechanism for the transport (e.g., whether the finite surface elevation or the advection is most important [Li and O'Donnell, 1997]). This fact, however, has been largely ignored when data from vessel-towed ADCPs were used to calculate the transport. The magnitude of transport due to the surface elevation can reach a/h [Ianniello, 1977] of the total transport, which can be about 10% at the Chesapeake Bay entrance. Therefore in a shallow estuary a complete study should also include the estimation of the surface elevation. It is possible to use a local tide gauge close to the study area, but the spatial variation of the amplitude and phase of the elevation can not be obtained from a single station.

It will be shown that under certain conditions it is possible to infer the tide of a given region by using the measured water depth from a vessel-towed ADCP along a transect in shallow coastal water. Obviously, when the water depth is large (~ 100 m), the variability of the water elevation may be less than the errors in the depth for the "same" position during different repetitions. Here we limit our study to water depths shallower than 30 m. This work is significant in that in tidally dominated shallow waters, vessel-towed ADCPs can provide useful information not recognized before to (1) resolve the spatial distribution of the tidal elevation, (2) describe the velocity in an Earth-coordinate system, (3) provide a complete picture of the tidal characteristics, that is, the phase difference between the surface elevation and velocity at each position, which enables us to calculate the total transport including the effect of the surface elevation, and (4) complement the conventional water elevation measurements from nearby tide gauges and from satellite altimeters which are more appropriate for global ocean problems. In section 2, we describe the data. In section 3, we describe the data analysis methodology. The data analysis results are presented in section 4. We further discuss our findings and present our conclusions in section 5.

2. Data

Dozens of cruises have been made between Cape Henry and Fishermans Island, at the entrance to the Chesapeake Bay (Figure 1), to collect current velocity data with an RD Instruments broadband 600 kHz ADCP using NOAA's ship *Ferrel* [e.g., Valle-Levinson et al., 1998]. This transect covers the 4 km wide Chesapeake Channel with a maximum depth of about 28 m; the 4.5 km wide, 10 m deep, Middle Ground; the 3.5 km wide Six-Meters Shoal; the 2.5 km wide North Channel with a maximum depth of 12 m; and the 1.5 km wide, 6 m deep, North Shoal (Figure 1). Both the Middle Ground and the Six-Meters Shoal have gentle bottom slopes, while the Chesapeake Channel and North Channel have relatively large depth variations. For our analysis we will use four cruises with repeated occupations of the transect on each cruise. The four cruises began in September 1996 and ended in November 1997 (Table 1). The ADCP was mounted on a catamaran and towed midship off the starboard side outside of the ship's wake. The ship speed was maintained at around 2.5 m/s, and the velocity data were averaged and recorded at 30 s intervals, which resulted in a horizontal resolution of about 75 m. Details of the ADCP data collection were provided by Valle-Levinson et al. [1998]. The water depth was directly measured by the four beams of ADCP. The mean value of the depths from the four beams was used in this analysis. According to RD Instruments, the maker of the ADCP, the "relative error" of the depth measurement is 1% of the total depth. Since the maximum depth in the Chesapeake Bay is about 30 m, the maximum "absolute error" of the ADCP is about 0.3 m, which is smaller than the average tidal range (~ 1 m). If other errors associated with the observations (e.g., navigational error or inaccurate ship track) are small enough, then the water depth measured from a vessel-towed ADCP in Chesapeake Bay should contain a clear signal of the tidal oscillation.

The vessel towing the ADCP attempted to remain close to the planned transect (Figure 2). We have chosen two parallel lines about 320 m apart on the sides of the planned transect as the across-transect boundaries within which the data are used in the subsequent analysis. The ship tracks were usually within the 320 m wide strip. Most meanderings and out-of-limit coordinates took place at the Chesapeake Channel due to ship traffic during the cruises, and at the ends of the transect where the ship turned. The ship tracks over the Middle Ground and the Six-Meters Shoal were usually

Table 1. Cruises

Date	Length (hour)	Repetitions
Sept. 1996	30	14
Feb. 1997	25	13
Sept. 1997	92	44
Nov. 1997	72	32+

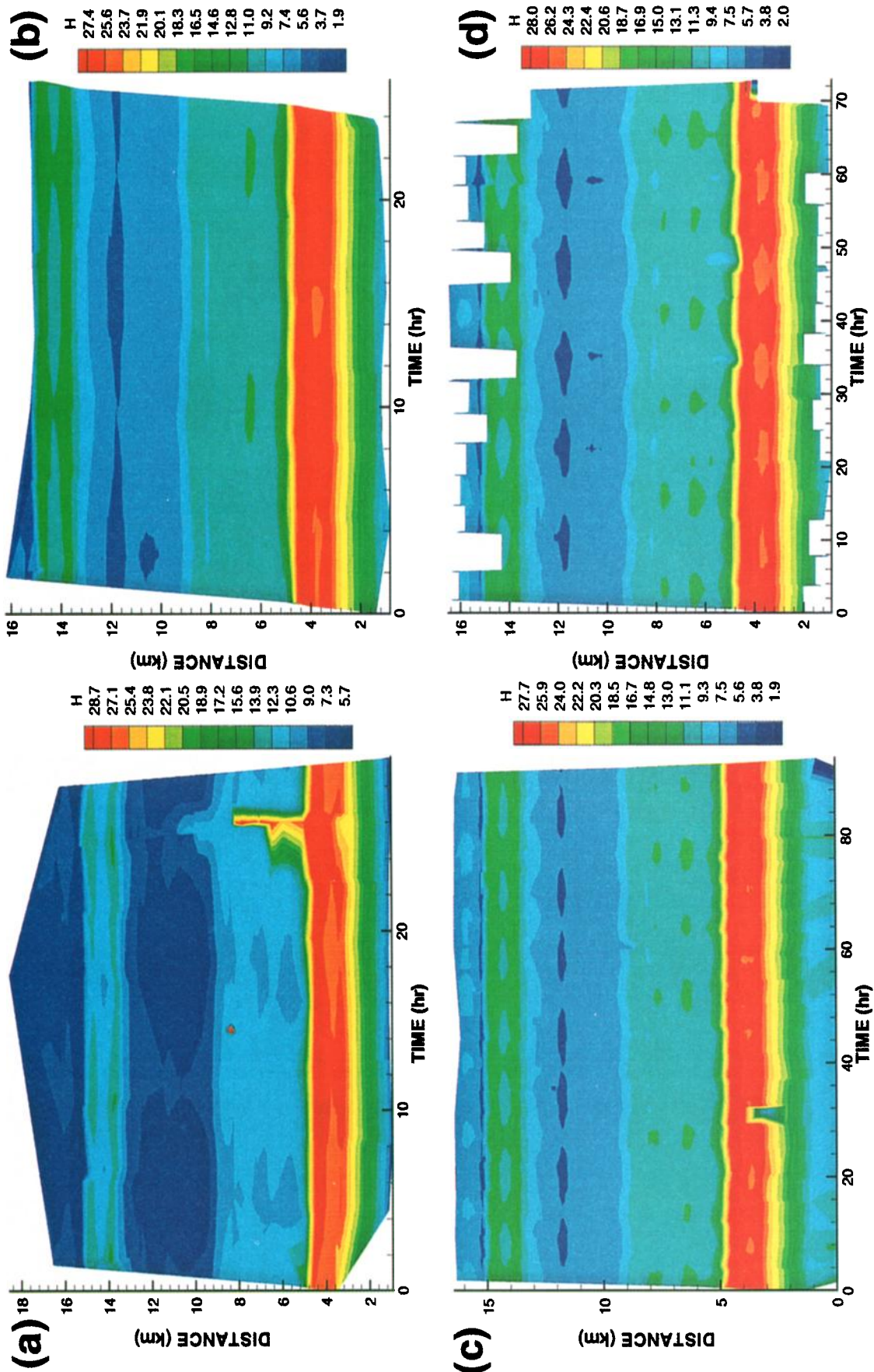


Plate 1. Temporal variation of water depth along the transect for the cruises of (a) September 1996, (b) February 1997, (c) September 1997, and (d) November 1997.

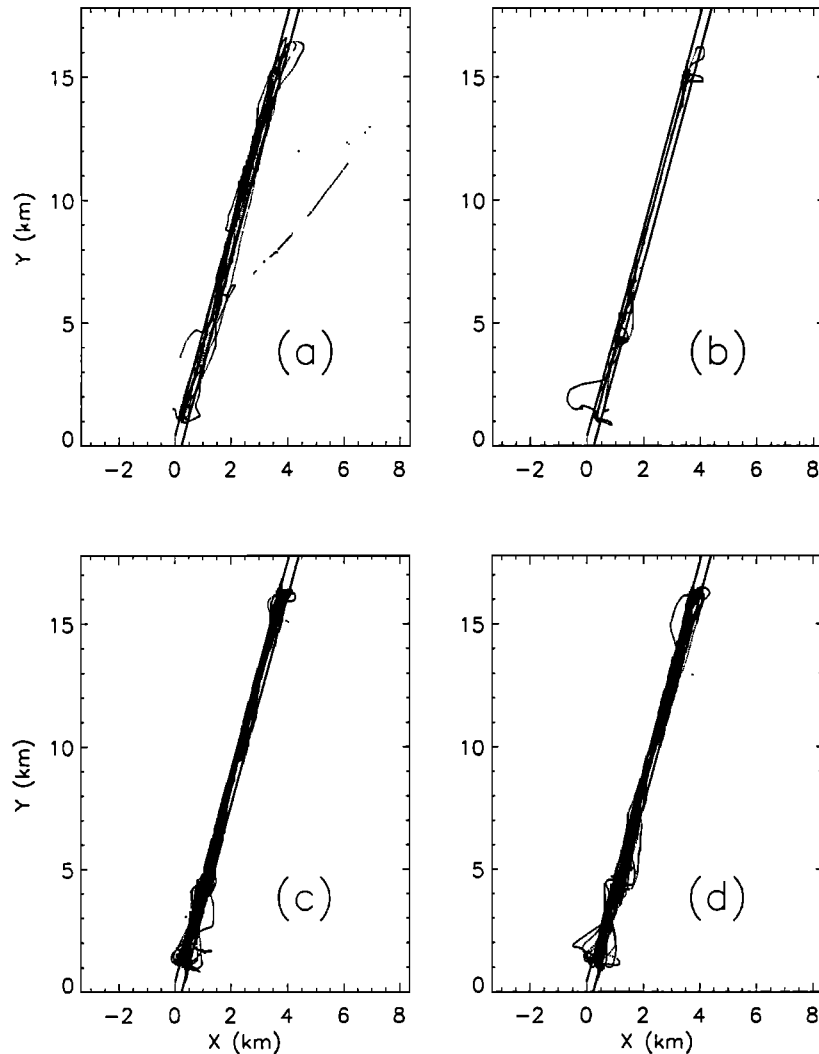


Figure 2. Ship tracks of the (a) September 1996, (b) February 1997, (c) September 1997, and (d) November 1997 cruises.

straight and within the boundaries (Figure 2). This 16 km long transect across the bay entrance is divided into 200 equal segments (or 80 m long each, which is close to the horizontal spatial resolution of 75 m determined by the ship speed and averaging interval), and the water depth within each segment was then grouped to obtain a time series. It is assumed that the depth variation within each segment is on average smaller than the spatially averaged temporal variability within the same segment. In other words, we distinguish only the temporal but not the spatial variability within the segment. The contour plots of the water depth time series (Plate 1) showed an apparent periodic pattern of the depth variation, particularly over Middle Ground and Six-Meters Shoal where the bottom slopes were small. In contrast, periodicities in the Chesapeake Channel appear to be less obvious. There may be two reasons for the differences: (1) the spatial variation of depth over the Chesapeake Channel was large, and (2) the ship track over the channel was sinuous; although the ship tracks were

within the selected boundary, they were more scattered in position than those elsewhere.

3. Data Analysis

In order to analyze the data quantitatively and determine if the data can be used to infer the surface elevation, we assume that the time-dependent total water depth h_t within any segment can be expressed as

$$h_t = \alpha_0 + \sum_{j=1}^M [\alpha_j \cos(\omega_j t) + \beta_j \sin(\omega_j t)], \quad (2)$$

in which α_j and β_j ($j = 0, 1, 2, \dots, M$) are harmonic constants, ω_j is the j th tidal frequency, t is time, and M is the total number of tidal frequencies selected. In matrix form, equation (2) is simply

$$H = Ax, \quad (3)$$

in which H is the depth vector composed of values mea-

sured at different times in a given segment along the transect, A is a matrix, and x is a vector of the harmonic constants, that is,

$$H = (h_1, h_2, \dots, h_N)^T, \quad (4)$$

$$\begin{aligned} x &= (\alpha_0, x_1, x_2, \dots, x_{2M})^T, \\ x_{2k-1} &= \alpha_k, x_{2k} = \beta_k, \\ k &= 1, 2, \dots, M, \end{aligned} \quad (5)$$

where T denotes the transpose of the vector, and

$$A = \begin{pmatrix} 1 & a_{1,1} & a_{1,2} & \cdots & a_{1,2M} \\ 1 & a_{2,1} & a_{2,2} & \cdots & a_{2,2M} \\ \vdots & & & & \vdots \\ 1 & a_{N,1} & a_{N,2} & \cdots & a_{N,2M} \end{pmatrix} \quad (6)$$

where N is the total number of observations and

$$\begin{aligned} a_{i,2k-1} &= \cos(\omega_k t_i), \quad a_{i,2k} = \sin(\omega_k t_i), \\ i &= 1, 2, \dots, N, \quad k = 1, 2, \dots, M. \end{aligned} \quad (7)$$

Since equation (3) is usually ill posed or overdetermined ($N \gg M$), we choose the least squares method to estimate the harmonic constants (the vector x). It can be readily shown that the best statistical estimate of x is

$$\hat{x} = (A^T A)^{-1} A^T H. \quad (8)$$

The error or the residual sum of squares is

$$R_{SS} = (H - A\hat{x})^T (H - A\hat{x}), \quad (9)$$

and the standard deviation (or the rms error) of the fitting and the coefficient of determination are, respectively,

$$\hat{\sigma} = \sqrt{\frac{R_{SS}}{N - (2M + 1)}} \quad (10)$$

and

$$R^2 = 1 - \frac{R_{SS}}{R_{HH}}, \quad (11)$$

in which R_{HH} is

$$R_{HH} = \sum_{i=1}^N \left(h_i - \sum_{j=1}^N h_j / N \right)^2. \quad (12)$$

Equation (11) is the fraction of variability of the water depth explained by the tidal constituents plus the mean, which is 1 minus the unexplained variability R_{SS}/R_{HH} . In the following section we present the results of harmonic and statistical analysis using equations (8), (10), and (11) for the water depth measured by the ADCP in each segment in the transect and discuss its spatial variability.

4. Results

In our application we include the M_2 semidiurnal ($T=12.42$ hours) and diurnal ($T=24$ hours) tidal constituents and a mean component for the total water

depth. The mean component represents the subtidal contribution, invariant in time, during each period of observation. Since the longest record (September 1997) presented here is only 92 hours, we can not distinguish N_2 , S_2 , and K_2 from M_2 , nor can we distinguish O_1 from K_1 , or P_1 . Adding N_2 , S_2 , K_2 , and O_1 to the harmonic analysis only superficially improves the fits by a maximum of 3%. At the majority of the positions the improvements are even smaller. At certain places, increasing the number of frequencies to the fits may even lower the quality of the fits because some of the frequencies are too close to each other. This may make the matrix (equation (7)) almost singular. Therefore the "semidiurnal tide" and "diurnal tide" here should be understood as $M_2+S_2+K_2+N_2$ and $K_1+P_1+O_1$, respectively.

Figure 3 shows the measured and fitted total depth time series at four positions along the transect. The four positions were chosen at the Chesapeake Channel, Middle Ground, Six-Meters Shoal, and North Channel (Figure 1), respectively. The fits for Chesapeake Channel and North Channel are relatively poor, while the fits at the Middle Ground and Six-Meters Shoal are much better. The Chesapeake Channel has more errors in the fits than does the North Channel.

Figures 4a - 4d show the proportion of variability of the water depth explained by the fits, as given by equation (11). Figure 4e shows the bathymetry and the locations where $R^2 \geq 0.7$. The fits to data from the four cruises exhibit strikingly similar characteristics. The fits with $R^2 \geq 0.7$ occur at five places: (1) the middle of the Chesapeake Channel, (2) most of the Middle Ground, (3) the Six-Meters Shoal, (4) the middle of the North Channel, and (5) the North Shoal. The best fits appear at the Six-Meters Shoal, where R^2 reaches almost 1 for September 1996, followed by those for February 1997 (0.98), November 1997 (0.95), and September 1997 (0.9). The R^2 values over Middle Ground are above 0.9 on average, except for September 1997 (0.87). In the deepest part of the Chesapeake Channel, the R^2 value reaches 0.97, 0.88, 0.78, and 0.90 for September 1996, February 1997, September 1997, and November 1997, respectively. The R^2 value over the middle of the North Channel is even higher than those from the Chesapeake Channel. The fits with $R^2 \leq 0.4$ occur mainly over the edges of the two channels. In addition, the R^2 values between Middle Ground and Six-Meters Shoal are smaller than adjacent positions, particularly during September 1997 (Figure 4c).

The semidiurnal and diurnal tidal amplitude of the temporal variation of the total depth or, equivalently, the surface elevation, and the standard deviation of the fits are shown in Figures 4f - 4i. Figure 4j is identical to Figure 4e. The along-transect variation of the tidal amplitude is small where $R^2 \geq 0.7$. Therefore the large variations of the semidiurnal and diurnal tidal amplitudes at the edges of the Chesapeake Channel, North Channel, and between the Middle Ground and

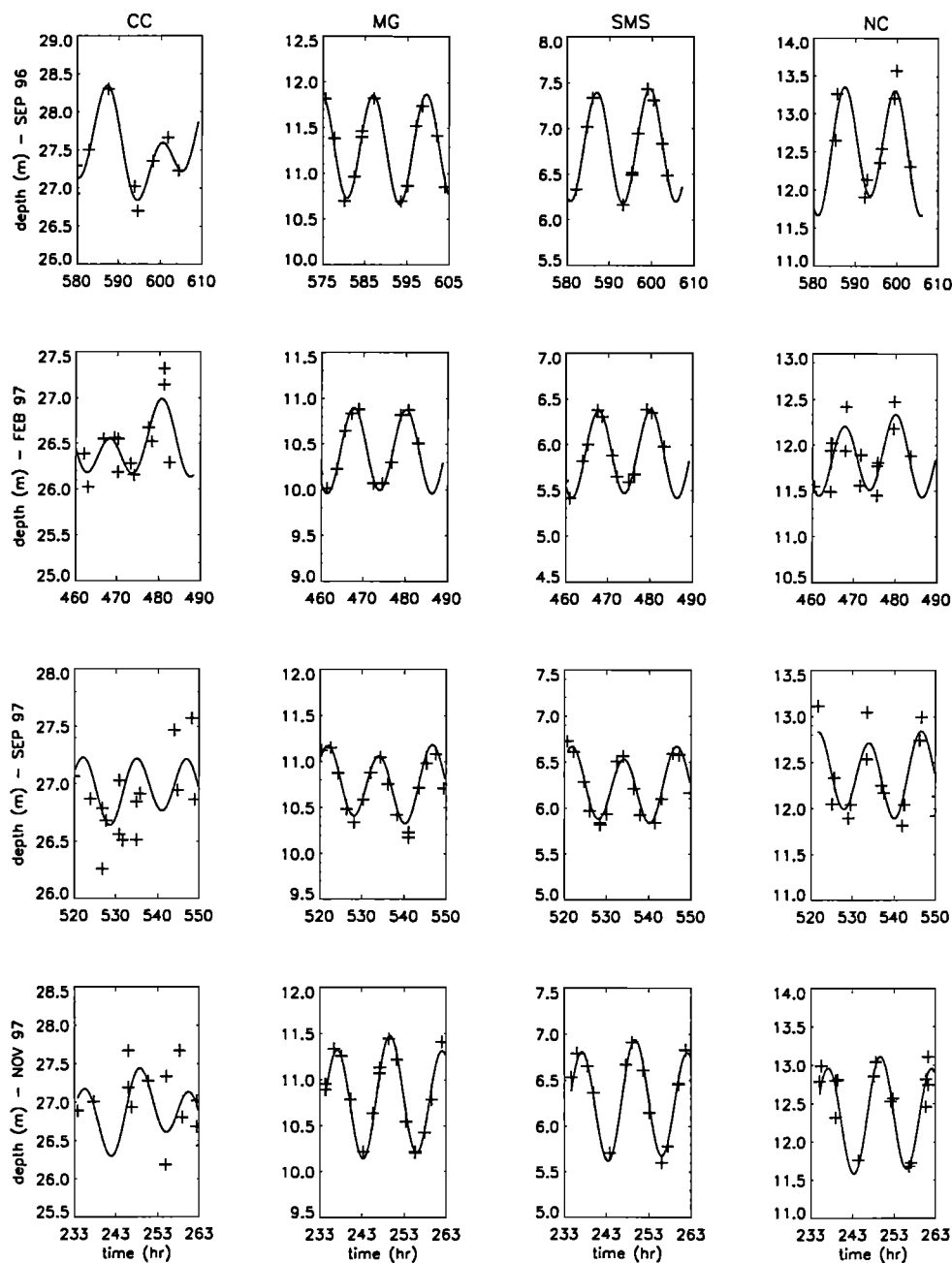


Figure 3. Measured (crosses) and fitted (lines) tidal variation of depth. The first, second, third, and last rows correspond to the September 1996, February 1997, September 1997, and November 1997 cruises, respectively. The left to the right columns correspond to positions in the Chesapeake Channel (CC), Middle Ground (MG), Six-Meters Shoal (SMS), and North Channel (NC), respectively.

Six-Meters Shoal are likely due to errors of the fits. These large variations also correspond to areas of large standard deviations and where $R^2 < 0.7$ (Figures 4f – 4i). Excluding those results with $R^2 < 0.7$, however, we still observe some consistent patterns of the spatial variation of amplitude and phase:

1. The semidiurnal tidal amplitude appears to have a slightly higher value over the North Shoal than that over the Chesapeake Channel. The phase difference between the elevation and velocity at the Chesapeake Bay

entrance is about 20° [Browne and Fisher, 1988], indicating that the tidal wave is roughly progressive there. Theoretically, a progressive Kelvin wave would produce an amplitude difference of about 13% across a 10 m deep 16 km long entrance at 37°N .

2. Some small-scale variations in amplitude (Figures 4f – 4i) may indicate some topographically trapped tidal waves. However, we may need more accurate observations to investigate this issue further.

3. The semidiurnal tidal variation of the depth (max-

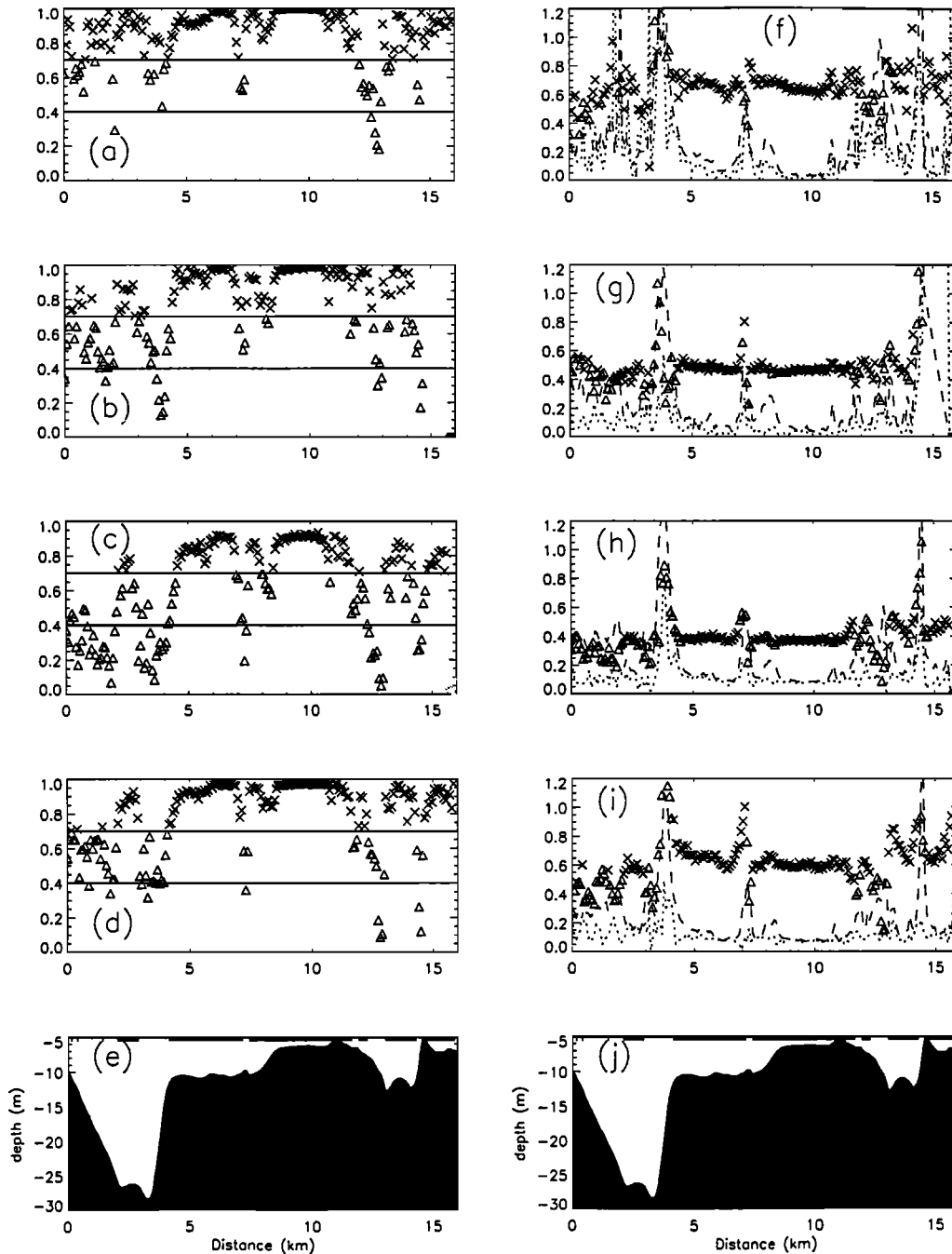


Figure 4. Results of harmonic analysis of depth along the transect for September 1996 (Figures 4a and 4f), February 1997 (Figures 4b and 4g), September 1997 (Figures 4c and 4h), and November 1997 (Figures 4d and 4i). Figures 4a-4d show R^2 , the proportion of variability of depth explained by the fitting. The crosses and triangles represent points where $R^2 \geq 70\%$ and $R^2 < 70\%$, respectively. Figures 4f-4i show the semidiurnal amplitude (with crosses and triangles corresponding to $R^2 \geq 70\%$ and $R^2 < 70\%$, respectively), diurnal tidal amplitude (dotted line), and the standard deviation (dashed line), all in meters. Figures 4e and 4j are identical and show the along-transect bathymetry and the positions where the fit explains 70% or more of the depth variation, denoted by the wide ticks at the surface.

imum 0.7 m) is dominant over the diurnal tidal variation, particularly during September 1996 and February 1997, when the diurnal amplitude was smaller than 0.1 m.

4. The standard deviations over Middle Ground and Six-Meters Shoal are uniformly small (≤ 0.1 m for the

most part). The diurnal tidal amplitude has a magnitude comparable to the standard deviation but nevertheless improves the fits by at least 10% at some locations.

In general, the better fits for September 1996 and February 1997 are due to the fact that these two records

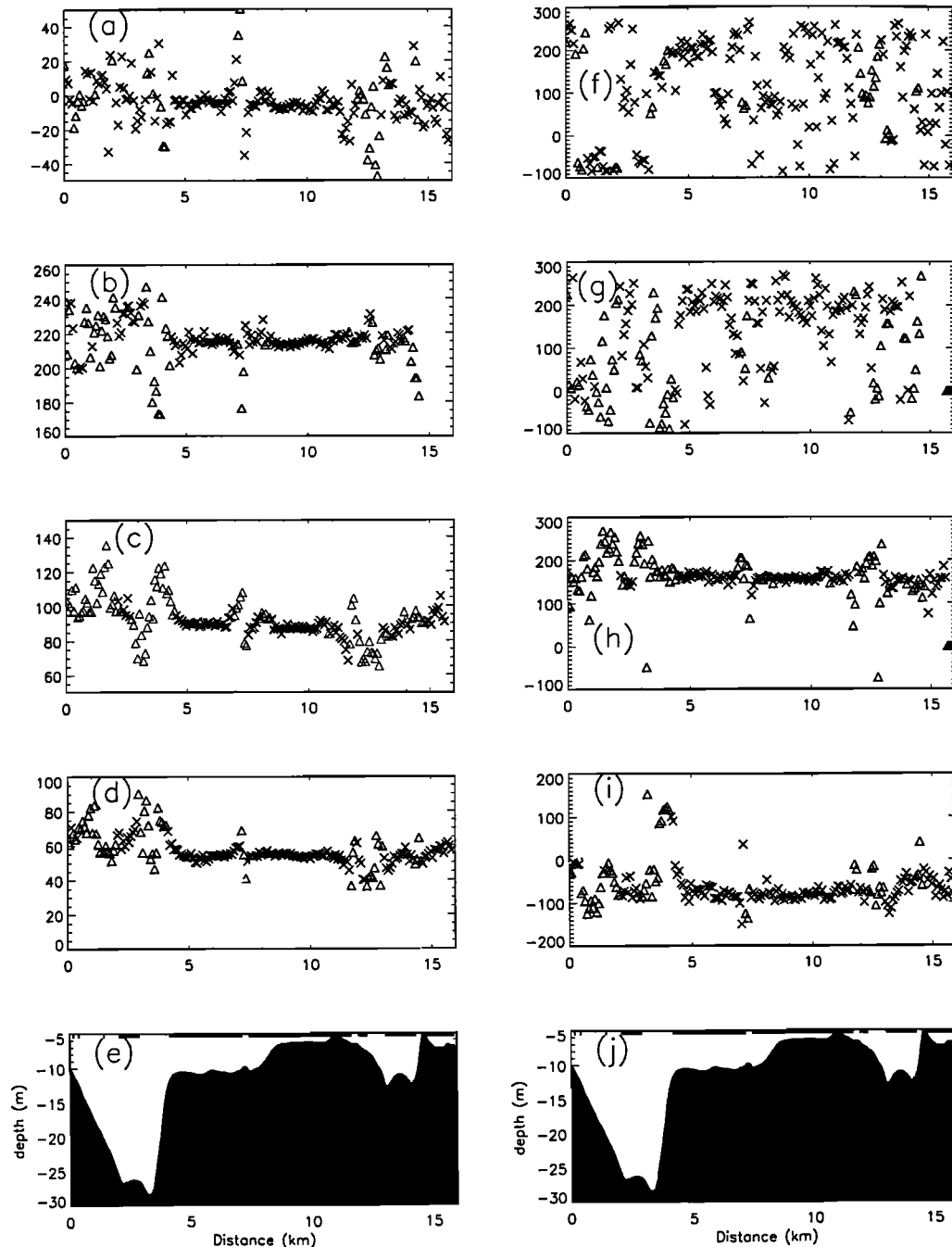


Figure 5. Results of harmonic analysis of depth along the transect (continued). Similar to Figure 4, except that here Figures 5a–5d show the phase (in degrees) of the semidiurnal tide and Figures 5f–5i show the phase of the diurnal tide (in degrees).

cover only two semidiurnal tidal cycles. Figure 4 also shows that where the fits are good ($R^2 \leq 0.7$), there is a noticeable difference in mean semidiurnal tidal amplitude from cruise to cruise. This is apparently the spring-neap variation.

Figure 5 shows the semidiurnal tidal phase (Figures 5a–5d) and the diurnal tidal phase (Figures 5f–5i) for the four cruises. Excluding the area where $R^2 < 0.7$ and with a few exceptions, the semidiurnal tidal phase is almost uniform along the transect with only a few degrees of variability. This is in contrast to the semi-

diurnal phase variation of tidal velocity along the same transect [Valle-Levinson *et al.*, 1998], which can reach up to 90° (3 hours). The difference is apparently due to the fact that most estuaries are elongated and any surface gradient will produce a restoring force of gravity to render the surface flat by way of dissipative surface waves. Li [1996] explained that phenomenon by a scaling analysis. Li [1996] and Li and Valle-Levinson [1999] further discussed it and presented some analytic solutions which showed large velocity gradients when the across-channel surface elevation had negligible spa-

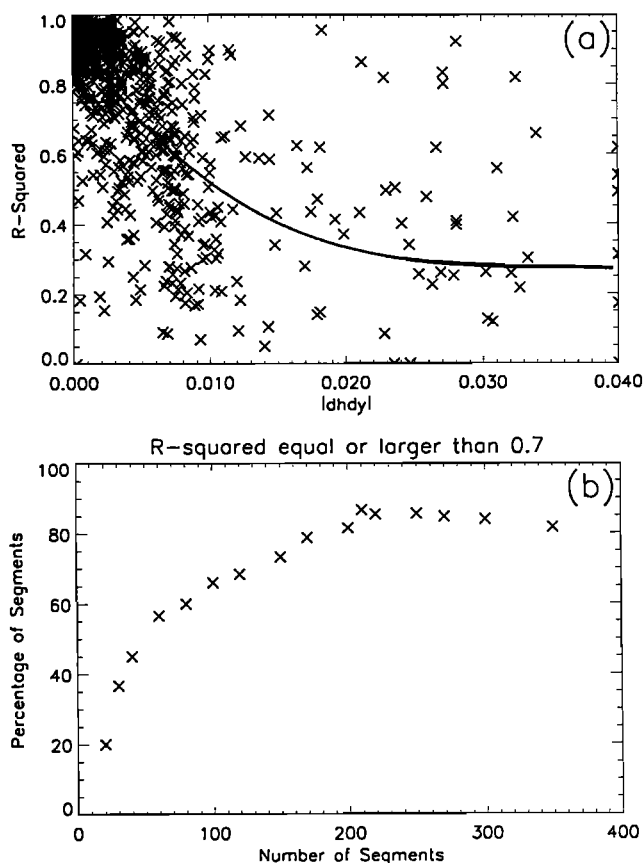


Figure 6. (a) The R^2 in relation to the magnitude of the bottom slope. The crosses are from ADCP, and the solid line is the fit of these data points to a third-order polynomial. (b) Percentage of segments with $R^2 \geq 0.7$ as a function of the number of segments along the transect.

tial variations. Again, in Figure 5 the positions with large variations of phase coincided with small R^2 and are probably due to errors associated with large bottom slopes. The diurnal tidal phase of the depth (Figures 5f - 5i) is more randomly distributed, especially for September 1996 and February 1997, which is consistent with the near-zero diurnal tidal amplitude for these two cruises (Figures 4f and 4g). In contrast, the diurnal phase for September 1997 and November 1997 exhibits smaller variation where $R^2 \geq 0.7$, consistent with the larger diurnal tidal amplitude for these two cruises (Figures 4h - 4i).

5. Discussion and Conclusions

5.1. Bottom Slope Versus R^2

The results suggest that the statistical characteristics of the harmonic analysis of the depth variation are position-dependent. Particularly, the larger the bottom slope is, the worse the fit appears to be. This can be better visualized by a plot of the R^2 values against the magnitude of the bottom slope $s = |\partial h / \partial y|$ (Figure 6a) in which y is the along-transect distance.

The observations (the crosses in Figure 6a) are fitted to a third order polynomial (the solid line in Figure 6a, $R^2 = a + a_1s + a_2s^2 + a_3s^3$), which shows a decrease of R^2 as the bottom slope increases. The large scatter of data points in Figure 6a suggests that there should be other factors, in addition to bottom slope, that affect the quality of the harmonic analysis. The ship speed is among these factors: For the same bottom slope, different ship speed may result in a different range of measured depths for the same time period. During the observations the ship speed fluctuated between 1 and 3.5 m/s. About 88% of the time the ship speed was between 1 and 3 m/s. Only 66% of the time was the ship speed above 2 m/s. In addition, the depth variation across the transect ($|\partial h / \partial x|$) may also affect the result. Even though the harmonic analysis of depth can be very different in statistical characteristics at different positions, our analyses show that about 66%, 56%, and 37% of the observations yield an R^2 larger than 0.7, 0.8, and 0.9, respectively. It can be seen from Figure 6 that $R^2=0.7$ corresponds to a mean bottom slope of about 0.006. Of the total length of the transect, 71% has a bottom slope smaller than 0.006. Therefore, excluding the observations over large bottom slopes or those with small R^2 values, about 60-70% of the measured depth by the ADCP during the four cruises presented here can be used to reliably infer the tidal elevation along the transect. The bathymetry of the Chesapeake Bay entrance is typical of many shallow ($h \leq 30$ m) estuaries with both relatively flat shoals and large slope over relatively deep channels. The method presented here can thus be a useful tool for the study of tides and transport in such shallow estuaries.

5.2. Effect of Segment Size

The segment (or grid) size may affect the quality of the harmonic analysis. Since the horizontal resolution of the observations is about 75 m on average (2.5 m/s \times 30 s), the total number of segments dividing the transect can not be much smaller or greater than $N = 16$ km / 75 m = 210 . For a small N the segment size is too big, and the depth range within each segment can be too large to allow a reliable detection of the tidal signal. For a large N , on the other hand, the segment size may be too small, and there may be too many time gaps between observations inside a given segment. By decreasing the N value from 200 to 80, we found that based on the four cruises, the percentage of fits with R^2 larger than 0.7, 0.8, and 0.9 decreased from 66%, 56%, and 37% to 52%, 42%, and 27%, respectively. Figure 6b shows the percentage of segments with $R^2 \geq 0.7$ in response to the change of the total number of segments for the September 1996 cruise alone. Calculations show that at around $N = 200$, that is, when the segment size is about the average horizontal resolution, the fits are optimal. It should be pointed out, however, that the segment size does not affect the general characteristics of the fits

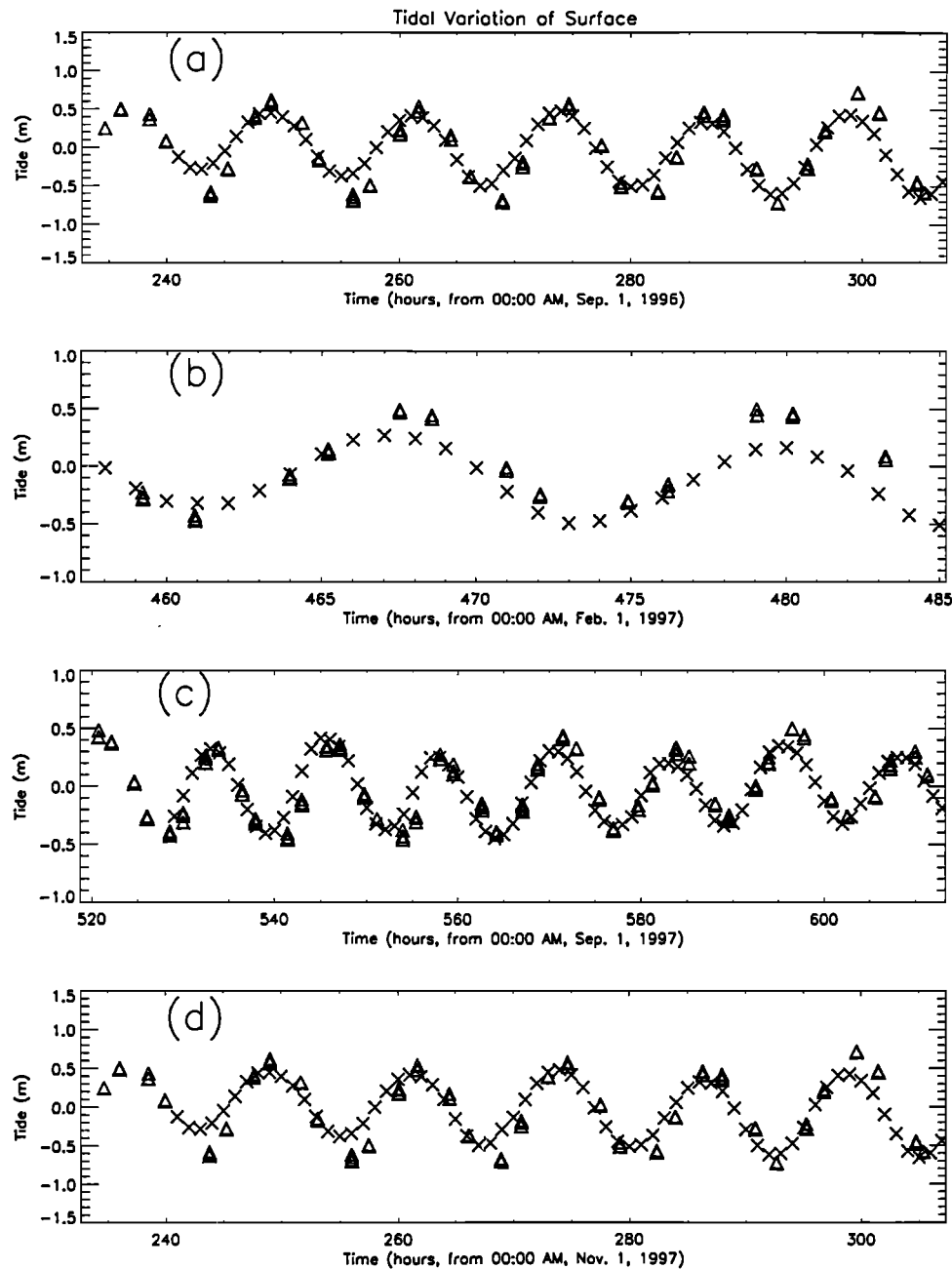


Figure 7. Comparison with NOAA's tide gauge observations. We have chosen the ADCP measurements from Six-Meters Shoal, where the fits are optimal, to compare with the station data. Data are for (a) September 1996, (b) February 1997, (c) September 1997, and (d) November 1997. Triangles are surface elevation inferred from water depth measured by the ADCP, and crosses are from NOAA data. The horizontal axis is time (UT) in hours from the beginning of the month of observations.

(e.g., amplitude and phase of the tide or the qualitative relationship between the slope and R^2).

5.3. Comparison With Station Data

To further test the reliability of this analysis, we now compare the present results with the NOAA's tide gauge observations (station 8638863) at the Chesapeake Bay Bridge and Tunnel (CBBT). The NOAA's tide station is located at $36^{\circ}58'N$, $76^{\circ}6.8'W$, with a mean depth

of about 9 m, over the edge of a channel, about 10 km west of the transect (Figure 1). The de-meaned observed tide from NOAA's CBBT station during the same time periods of the cruises is compared with that obtained from the ADCP measurements (Figure 7) over Six-Meters Shoal, where R^2 is almost 1. Both amplitude and phase from the ADCP are consistent with those from the tidal gauge. On a number of occasions, the ADCP results appear to have a slightly larger amplitude

(particularly for February 1997). The difference could be a result of a spatial variation in tide, considering that the Coriolis effect across a 16 km transect may cause a 13% decrease of amplitude from north to south as discussed earlier in section 4. The NOAA's CBBT station is further inside the bay and has a slightly smaller tidal amplitude on average and is less subject to wind effect [Browne and Fisher, 1988].

5.4. Conclusions

In conclusion, by a harmonic and statistical analysis of data from a vessel-towed ADCP, we have obtained semidiurnal and diurnal tidal amplitudes and phases along a 16 km transect across the Chesapeake Bay entrance with a horizontal spatial resolution of about 80 m. Both the amplitudes and phases exhibit only small variations along the transect. The slight increase of the semidiurnal tidal amplitude at the north end appears to be consistent with the Coriolis effect. Our study has shown that at places with bottom slopes less than 0.006 and with an average ship speed of 2.5 m/s, tidal elevation can be reliably calculated from a towed ADCP. At least 70% of the variability of the depth can be explained by semidiurnal and diurnal tides if the bottom slope is 0.006 or smaller. This provides a convenient alternative of obtaining tides in shallow estuaries using a vessel-towed ADCP while velocity profiles are recorded at the same time. The spatial distribution of tidal elevation along the transect can then be obtained with a horizontal resolution that can be achieved only by densely moored ADCPs. Future studies can benefit from this work since the tidal elevation obtained from a vessel-towed ADCP can be used to transform the vertical coordinate to one with a fixed reference level to minimize errors of the velocity analysis. Furthermore, the spatial distributions of the phase difference between the elevation and velocity and the amplitude of the elevation can be used to correctly estimate the total transport to the second order.

Acknowledgments. This work was funded by the U.S. Minerals Management Service under cooperative agreement 14-35-0001-30807 and by the NOAA Office of Sea Grants, under grant NA56RG0489 to the Virginia Graduate Marine Science Consortium and Virginia Sea Grant College Program. Ship time on the NOAA ship *Ferrel* was provided by the National Sea Grant College Program. The authors would like to thank G. Marmorino and an anonymous reviewer for their review comments which helped improve the

manuscript. We appreciate the cooperation from the crew of the *Ferrel* under the able command of LCDRs S.D. McKay and I. Byron. We also appreciate the technical support of R.C. Kidd in every cruise and the participation and help of L. Heilman, K. Holderied, C. Reyes, R. Ellison, B. Fach, M. Gruber, G. Jiang, S. Kibler, J. Klinck, R. Locarnini, T. McCarthy, M. Moore, S. Ouelette, M. Paraso, B. Parsons, C. Reiss, D. Ruble, J. She, and K. Wong on different cruises. The NOAA's tide observations at the CBBT were obtained from NOAA's web page at <http://co-ops.nos.noaa.gov/>.

References

- Browne, D.R., and C.W. Fisher, Tide and tidal currents in the Chesapeake Bay, *NOAA Tech. Rep. NOS OMA3*, 84pp., Natl. Oceanic and Atmos. Admin., Silver Spring, Md., 1988.
- Brubaker, J. M., and J. H. Simpson, Flow convergence and stability at a tidal estuarine front: Acoustic Doppler current observations, *J. Geophys. Res.*, *104*, 18,257-18,268, 1999.
- Ianniello, J.P., 1977, Tidally induced residual currents in estuaries of constant breadth and depth, *J. Mar. Res.*, *35*, 755-785, 1977.
- Li, C., Tidally induced residual circulation in estuaries with cross channel bathymetry, Ph.D. dissertation, 242 pp., University of Connecticut, Storrs, 1996.
- Li, C., and G. Fang, Some spatially integrated time-averaged identities for fluids, *Chin. J. Oceanol. and Limnol.*, *17*, 315-330, 1999.
- Li, C., and J. O'Donnell, Tidally driven residual circulation in shallow estuaries with lateral depth variation, *J. Geophys. Res.*, *102*, 27,915-27,929, 1997.
- Li, C., and A. Valle-Levinson, A two-dimensional analytic tidal model for a narrow estuary of arbitrary lateral depth variation: The intratidal motion, *J. Geophys. Res.*, *104*, 23,525-23,543, 1999.
- Lwiza, K.M.M., D.G. Bowers, and J.H. Simpson, 1991, Residual and tidal flow at a tidal mixing front in the North Sea, *Cont. Shelf Res.*, *11*, 1379-1395, 1991.
- Phillips, O.M., *The Dynamics of the Upper Ocean*, Cambridge Univ. Press, 336 pp., New York, 1977.
- Valle-Levinson, A., C. Li, T. Royer, and L. P. Atkinson, Flow regimes in lower Chesapeake Bay, *Cont. Shelf Res.*, *18*, 1157-1177, 1998.
- L. P. Atkinson, T. C. Royer, and A. Valle-Levinson, Center for Coastal Physical Oceanography, Department of Ocean, Earth, and Atmospheric Sciences, Crittenton Hall, Old Dominion University, Norfolk, VA 23529. (e-mail: arnoldo@ccpo.odu.edu)
- C. Li, Skidaway Institute of Oceanography, 10 Ocean Science Circle, Savannah, GA 31411. (e-mail: chunyan@skio.peachnet.edu)

(Received December 21, 1999; revised May 22, 2000; accepted July 26, 2000.)